Bulgarian Chemical Communications, Volume 43, Number 4, (pp. 489 - 501) 2011

Lanthanide oxide doped titania photocatalysts for degradation of organic pollutants under UV and visible light illumination

D. Tz. Dimitrov*, M. M. Milanova, R. P. Kralshevska

Department of General and Inorganic Chemistry, Faculty of Chemistry, University of Sofia, 1, J. Bourchier Blvd., Sofia 1164, Bulgaria

Received November 2, 2010; Revised January 5, 2011

The main goal of this short review is to present the most valuable attempts that have been made in the past decades to shift the absorption of TiO_2 from UV- to the visible-light region by lanthanide doping. In order to understand the other factors by which doping of TiO_2 with lanthanides can increase the photocatalytic activity under solar irradiation, the first short chapter is devoted to the physical mechanisms responsible for the degradation of organic pollutants by lanthanide oxide doped titania under UV-light exposure. This aspect has been studied for a long time and is better understood. The second chapter deals with the same features, but extended for the visible-light exposure of catalysts. The most typical observations for bathochromic shift, effect of co-doping and organic dye sensitizing on the photocatalytic activity of lanthanide oxide doped titania are considered in detail.

Key words: photocatalysts, titania, lanthanides-doped titania, visible light.

INTRODUCTION

The heterogeneous photocatalysis based on oxide semiconductors is a promising technology for remedying environmental pollution and solving energy depletion and has become one of the most active research fields in recent years. So far, researchers have developed many materials that have the potential to act as photocatalysts for a wide range of applications including TiO_2, WO_3, $SrTiO_3$, α-Fe_2O_3, ZnO and $NaBiO_3$. Among them, TiO_2 has proven to be a benchmark catalyst for detoxification of organic pollutants [1-4]. The photoexcitation of a semiconductor leads to the formation of an electron-hole pair. The excited-state conduction band electrons can: recombine with the holes and dissipate the input energy; get trapped in surface states; react with electron donors and electron acceptors adsorbed on the semiconductor surface [5].

In particular, because of their unique 4*f*-electronic configuration and spectral characteristics, lanthanides are ideal dopants for modifying the crystal structure, electronic structure, optical properties and surface adsorption of TiO_2 and forming a series of novel promising photocatalysts. On the other hand, as a group of elements that both resemble each other and show particular differences between them, lanthanides provide an opportunity for an in-depth study of the electronic structure that can influence the performance of TiO_2 photocatalysts [6]. However, as a wide band gap oxide semiconductor (E_g = 3.23 eV), anatase TiO_2 shows a photocatalytic activity only under UV-light irradiation ($\lambda < 384$ nm), which accounts for only a small fraction of the solar energy (~5%). The sun is an abundant source of photons, where visible light accounts for a large fraction of spectrum (~45%) [7]. Therefore, how to effectively utilize sunlight is the most challenging subject for extensive application of TiO_2. The main goal of the present article is to consider the most important attempts that have been made in past decades to shift the TiO_2 absorption from the UV region to the visible-light region. In order to understand all factors that can increase the photocatalytic activity under solar irradiation, the first short part of this review is devoted to the physical mechanisms responsible for the degradation of organic pollutants by lanthanide oxide doped titania under UV-light exposure.

1. PHYSICAL MECHANISMS RESPONSIBLE FOR THE DEGRADATION OF ORGANIC POLLUTANTS BY LANTHANIDE OXIDE DOPED TITANIA UNDER UV-LIGHT EXPOSURE

1.1 Enhancing of the photocatalytic activity of TiO_2 powder by suppressing electron-hole

---

* To whom all correspondence should be sent:
E-mail: DTsenov@wmail.chem.uni-sofia.bg

recombination with trapping of photogenerated electrons at the interface

Li *et al.* [8] have studied the effect of electrons, shallowly trapped by Gd^{3+} in nanocrystalline $La_{1.5}Gd_{0.5}Ti_2O_7$ solid solution and in Gd^{3+}-doped TiO_2, on the photocatalytic activity in the liquid phase. They claim that the half-filled *f*–shells of Gd^{3+} ions play a mechanistic role because it is more stable and when such a configuration is destroyed, it has a strong tendency to return to the original stable state. This particular characteristic of a dopant ion with a half-filled electronic configuration can promote the charge transfer and efficiently separate the electron–hole pairs by shallowly trapping electrons. Even though other metal ions can also trap the photo-excited electrons, the detrapping is more difficult on these ions.

Rengaraj *et al.* [9] have discovered the synergetic effect of neodymium ions deposited on the TiO_2 surface, which behave as sites where electrons and sacrificial electron donors such as formic acid accumulate. The transfer of photo-induced electrons from the TiO_2 conduction band to the metallic Nd particles at the interface is thermodynamically possible because the Fermi level of TiO_2 is higher than that of Nd metal [10].The proposed mechanism of the effect of both Nd particles and formic acid added as a hole scavenger is shown in Fig. 1.

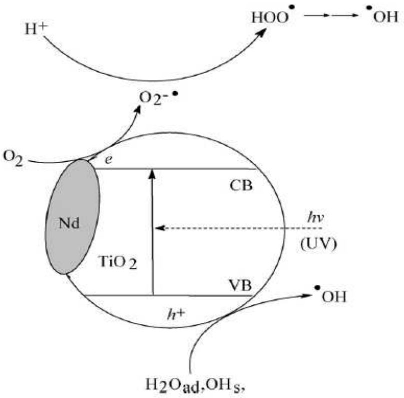

Fig. 1. Mechanism of the photocatalytic reaction on a Nd–TiO_2 catalyst under UV [9].

The metallic Nd particles at the interface will act as electron traps, enhancing the electron–hole separation and the subsequent transfer of trapped electrons to the adsorbed O_2 or Cr(VI) acting as an electron acceptor. This can be explained by the surface electronic effect induced by neodymium. This reaction enables the positive photoholes p^+ to react with adsorbed OH^- species in order to create $^\bullet OH$ radical, as shown in the sequence of Eqs. (1-3):

$$(TiO_2) + h\nu \rightarrow e^- + p^+ \tag{1}$$

$$Nd + e^- \rightarrow e_{Nd}^- \tag{2}$$

$$OH^- + p^+ \rightarrow {}^\bullet OH \tag{3}$$

The $^\bullet OH$ species formed from the holes will be accepted by HCOOH specially added for that purpose (Eq. (4)):

$$^\bullet OH + HCOOH \rightarrow \text{intermediates} \rightarrow CO_2 + H_2O \tag{4}$$

By this way HCOOH suppresses the electron–hole recombination process and increases the reduction efficiency. In the presence of formic acid, the Cr(VI) reduction reaction can be described as follows:

$$Cr_2O_7^{2-} + 14H^+ + 6e^- \rightarrow 2\,Cr^{3+} + 7H_2O \tag{5}$$

In this reaction, 1 mol of Cr(VI) requires 3 mol of electrons to be reduced to Cr(III), which needs an equivalent of 3 mol of HCOOH to scavenge the holes. The enhanced reduction of oxygen through better electron-hole separation in Nd–TiO_2 particles compared to pure TiO_2 increases the rate of HCOOH degradation while simultaneously increasing the rate of reduction of Cr(VI).

Yang *et al.* [11] have studied the photocatalytic activity of CeO_2/TiO_2 mixed oxide nanoparticles. They claim that the Ce^{4+}/Ce^{3+} redox couple increases the separation of electron-hole pairs. Doped cerium only may be present as the so-called second phase on the surface of TiO_2. CeO_2 can trap photo-generated electrons at the interface while reducing to Ce^{3+} according to the reaction (6):

$$e^- + Ce^{4+} \rightarrow Ce^{3+} \tag{6}$$

In this case, the role of Ce^{4+} is the removal of electrons from electron–hole recombination sites with simultaneous production of oxidizable species.

Mele *et al.* [12] have used lanthanide diphthalocyanine sensitizers on a polycrystalline anatase TiO_2 surface. These sensitizers work because of the positions of conduction and valence band energy levels of anatase TiO_2 relative to the redox potentials of the sensitizers allow charge transfer by injection of an electron from the excited sensitizers to the conduction band of TiO_2 and from the conduction band of TiO_2 to the sensitizers.

Jiang *et al.* [13] have studied TiO_2 composite nanoparticles doped with low amount of Yb^{3+}; the doping increases the number of hydroxyl groups on the TiO_2 surface because Ti^{4+} replaces Yb^{3+} in the

Yb_2O_3 crystal lattice and creates a charge imbalance. In order to restore the charge balance, more hydroxide ions will be adsorbed on the surface, which could enhance the lifetime of electron-hole pairs.

Ökte and Yılmaz [14] have investigated the synergy between ZSM-5, TiO_2 and La_2O_3 of lanthanum loaded TiO_2-ZSM-5 photocatalysts where TiO_2 and La_2O_3 nanoparticles are dispersed on the support surface. The benefit of La^{3+} ion incorporation is due to the capability of these ions to trap electrons, inhibit electron–hole recombination reactions and concentrate pollutant molecules on the catalyst surface. ZSM-5 acts as a hole trap (ZSM is abbreviation for Zeolite Sieve of Molecular porosity). This is possible because the high Si/Al ratio in ZSM-5 presents a limited number of Lewis acid sites in the framework. This property decreases the electron-delocalizing ability, but simultaneously allows capturing of photogenerated holes of TiO_2.

1.2 Enhancing of the photocatalytic activity of TiO_2 powder caused by the different effect of mesoporous walls

Peng *et al.* [15] have suggested that the presence of lanthanum ions in the TiO_2 mesostructure increases the photoactivity due to the larger surface area and more active sites for combining with molecules of the pollutant. The high degree of crystallinity also plays an important role in the photoactivity of TiO_2.

Zhao *et al.* [16] have shown that the absorption edge of TiO_2 shifts to the visible light range and the band-gap narrows, when TiO_2 is doped with Nd^{3+}. The Nd species are distributed in the bulk of nanoparticle instead of concentrating on its surface. Density functional theory calculations are used to interpret the narrowing of the band-gap. The density of states (DOS) profiles of the undoped TiO_2 and Nd^{3+}-doped anatase TiO_2 are shown in Fig. 2. The calculated value of the band-gap for undoped TiO_2 is 3.20 eV, which is in good agreement with the experimental value of 3.22 eV. The band-gap is formed between the O 2***p*** orbitals and Ti 3***d*** orbitals.

The main contribution to the valence band comes from O 2*p* orbitals, while the states at the conduction band are predominantly Ti 3*d* orbitals. A $NdTi_3O_8$ super cell models the Nd^{3+}-doped anatase with Nd atoms in the substitutional sites. The DOS for this structure is shown in Fig. 2 b with a much smaller band-gap value (1.93 eV) calculated. Obviously, the existence of DOS of Nd 4*f* orbitals means that some electronic states are introduced into the band-gap of TiO_2 by Nd 4*f* electron levels located close to the lower edge of conduction band to form new LUMO (lowest unoccupied molecular orbitals). Consequently, the photoexcited electron for Nd-doped material can be transferred from O 2*p* to Nd 4*f* instead of Ti 3*d*, which is different from the situation of undoped TiO_2.

1.3 The effect of co-doping on the photocatalytic activity

Shi *et al.* [17] have found a marked improvement of the photocatalytic activity of TiO_2 by co-doping with Fe^{3+} and Ho^{3+}. Fe^{3+}-doping improves the photoutilization of TiO_2 and generates more electron–hole pairs under photoirradiation, which helps to improve the photocatalytic activity of TiO_2.

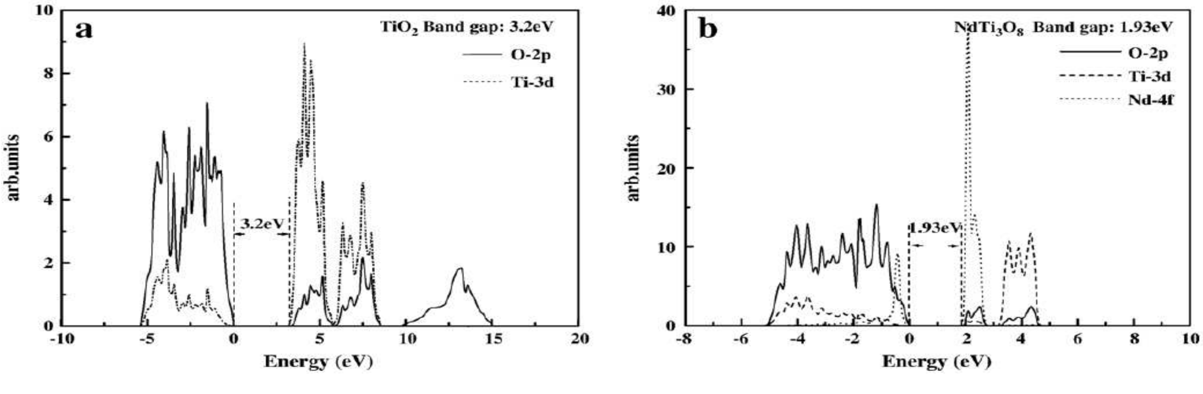

Fig. 2. Theoretically calculated density of states for undoped (a) and Nd-doped (b) TiO_2 [16].

The crystal expansion and matrix distortion of TiO_2 caused by Ho^{3+}-doping creates oxygen vacancies, which generate shallow energy states in the bottom of conduction band and serve as electron trap sites in nanocrystalline TiO_2. Meanwhile, shallow energy states introduced by the rare earth ions in the top valence band serve as hole trap sites. The separation of charge carriers is attributed to such trapping. Subsequently, the charge carriers transfer to the surface of photocatalyst to cause there redox reactions so that the photocatalytic activity of doped TiO_2 is promoted. When both Fe^3+ and Ho^{3+} are co-doped into the nanocrystalline TiO_2 particles, a synergistic effect will be produced. Fe^{3+}-doping broadens the absorption profile, improves the photoutilization of TiO_2, and thereby generates more electron–hole pairs. Ho^{3+}-doping prevents the increase of grain sizes, leads to a crystal expansion and matrix distortion and retards the recombination of photoexcited charge carriers. The photocatalytic activity of TiO_2 co-doped with Fe^{3+} and Ho^{3+} is markedly improved.

1.4 The effect of intrinsic surface properties on the photocatalytic activity

Zhang *et al.* [18] have investigated the poperties of $Dy_2Ti_2O_7$ prepared by two different methods: citric-acid sol–gel soft chemistry and solid state reaction route. $Dy_2Ti_2O_7$ nanocrystals prepared by the citric acid method have an oxygen content that is much lower than the theoretical value; the oxygen-deficiency on the $Dy_2Ti_2O_7$ surface is about 40%. This oxygen deficiency helps the catalyst to absorb more O_2 and is very benificial to achieve a good photocatalytic activity. Both the morphology and the degree, by which it can be dispersed, are quite different from those of samples produced by the solid state reaction. The $Dy_2Ti_2O_7$ crystals of samples obtained by the citric acid method are quadrilateral and have a good dispersibility, while the average crystal size is about 50 nm. It is very difficult to identify the morphology of $Dy_2Ti_2O_7$ produced by the solid state reaction and its dispersibility is quite low. The BET surface area of $Dy_2Ti_2O_7$ prepared by the citric acid method is 25 m^2/g, which is much larger than that of samples prepared by traditional solid state reaction (2 m^2/g) and other soft chemistry routes. The good physical properties of the sample obtained by the citric acid method result in a better photoactivity than that of the sample prepared by solid state reaction. For the first, the photodegradation of methyl orange is 98.6% within 60 min, whereas for the second, the degree of decomposition is only 16.0%.

2. PHYSICAL MECHANISMS RESPONSIBLE FOR THE DEGRADATION OF ORGANIC POLLUTANTS BY LANTHANIDE OXIDE DOPED TITANIA UNDER VISIBLE-LIGHT EXPOSURE

The effects of lanthanide doping on the electronic structures and optical properties of anatase TiO_2 are studied by Zhao and Liu [6]. They presented electronic structures and optical properties of pure anatase TiO_2 and lanthanide-doped TiO_2, based on calculations of the crystal structures. The results indicate that the lanthanide doping could remarkably improve the photocatalytic activity of TiO_2, and that the effect of improvement is sensitive to the atomic electronic configuration and ionic radius. Most lanthanide doping could narrow the band gap of TiO_2, so the fundamental absorption edges shift to the visible light region and simultaneously maintain strong redox potentials. In terms of the correlation of electronic structure and optical properties, the ref. [6] describes that there are three kinds of electronic transitions in lanthanide-doped TiO_2: intraband transition in lanthanide 4***f*** states, interband transition between O p_π states and lanthanide 4***f*** states and interband transition between IELs and valance band maximum or conduction band minimum (IELs is abbreviation for imputity energy levels).

2.1 Shift of the absorption from UV-light region to visible-light region by lanthanide doping

Parida and Sahu [19] have found a high photocatalytic activity for the reduction of hexavalent chromium and methylene blue degradation under visible light by La^{3+}-TiO_2 containing 0.4 mol% lanthanum, prepared by incipient wetness impregnation method and activated at 400°C. The photocatalytic activity of TiO_2 doped with lanthanides is shifted to the visible part of the spectrum (bathochromic shift). It was observed (see Fig. 3) that the absorption edges of La^{3+} doped TiO_2 shift slightly towards a longer wavelength (red shift) compared to that of pure TiO_2, for which the samples are active under visible light of the solar spectrum.

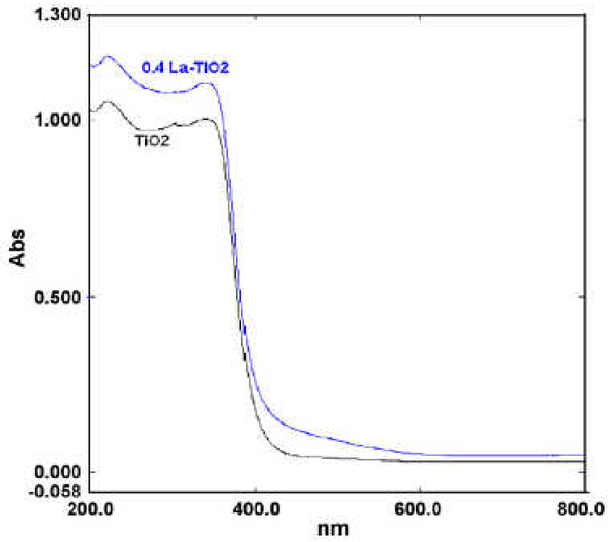

Fig. 3. UV–vis spectra of pure and La^{3+} doped TiO_2 [19].

Xiao *et al.* [20] have studied the visible light photocatalytic decomposition of methylene blue by 0.5 mol% Sm^{3+} doped TiO_2 produced by sol-gel auto-combustion synthesis. To investigate the optical absorption properties of their catalysts, they have examined the diffuse reflectance spectra (DRS) of TiO_2 and Sm^{3+}-doped TiO_2 in the range of 220–850 nm. They have found that while TiO_2 has no absorption in the visible region (>400 nm), Sm^{3+}-doped TiO_2 shows a significant absorption between 400 and 500 nm, which increases with increasing the samarium ion content. The photocatalytic activity of Sm^{3+}-TiO_2 is higher than that of undoped TiO_2, which is consistent with the larger specific surface area of Sm^{3+}-TiO_2 compared to undoped TiO_2. However, it is noticeable that the larger specific surface area of Sm^{3+}-TiO_2, resulting from a higher samarium ion dosage does not lead to a higher photocatalytic activity, which might be limited by a lower separation efficiency of electron–hole pairs.

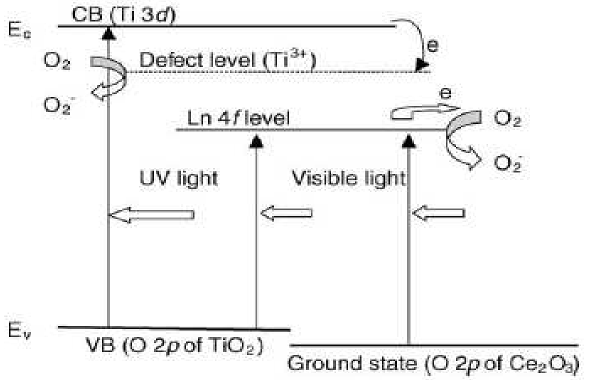

Fig. 4. The photoluminescence emission mechanmisms of TiO_2 and Ce^{3+}–TiO_2 catalysts at 77 K [21].

Li *et al.* [21] have found enhanced photocatalytic activity of Ce^{3+}–TiO_2 prepared by a sol–gel process for the degradation of 2-mercaptobenzothiazole in aqueous suspension for odor control. They have investigated the optical absorption properties of TiO_2 and Ce^{3+}–TiO_2 catalysts in the range of 220–850 nm and have found that while TiO_2 has no absorption in the visible region (>400 nm), Ce^{3+}–TiO_2 has a significant absorption between 400 and 500 nm, which increases with increasing the cerium content. CeO_2 is a n-type semiconductor with a band gap of about 3.2 eV [22,23]. Therefore, the absorption at 400–500 nm can not be attributed to CeO_2, but should rather be due to Ce_2O_3. In contrast to the closed shell of Ce^{4+}-ion ($4\boldsymbol{f}^{0}$), the Ce^{3+}-ion possesses a single optically active electron with the ground-state configuration in the $4\boldsymbol{f}^{1}$-orbital. Within this configuration, there are only two electronic levels, the $^2F_{7/2}$ excited state and the $^2F_{5/2}$ ground state. The $4\boldsymbol{f}$–$4\boldsymbol{f}$ transitions attributed to Ce^{3+} can only be observed in the infrared spectral region. However, Ce^{3+} has a first state configuration $5\boldsymbol{d}^{1}$ that is rather close in energy. The electronic dipole transitions $4\boldsymbol{f}^{1} \leftrightarrow 5\boldsymbol{d}^{1}$ may occur in either the UV or visible region. Based on the valence band of Ce^{3+}–TiO_2 as determined by XPS, the authors propose that electron hole pairs are generated in both types of catalysts (Ce^{3+}-TiO_2 and Ce_2O_3) by two mechanisms shown in Fig. 4. According to Eq. (7) , an electron can be excited from the valence band of Ce^{3+}–TiO_2 into the Ce 4 ***f***-level when the energy of the photon is more than ($\boldsymbol{E_{Ce4f}} - \boldsymbol{E_v}$). Equation (8) shows the excitation of an electron from the ground state of Ce_2O_3 into the Ce 4 ***f***-level.

Therefore, the red shift of the absorption edge for Ce^{3+}–TiO_2 is explained by the following two reactions. The Ce 4***f*** levels may play a crucial role in generating electron-hole pairs under visible light illumination.

$$Ce^{3+}-TiO_2 + h\nu \rightarrow e^- + h^+ \quad (7)$$

$$Ce_2O_3 + h\nu \rightarrow e^- + h^+ \quad (8)$$

The optimal dosage of cerium under visible light illumination is found to be 0.7%, while for UV illumination it is 1.2%. Ikeda *et al.* [24] have proposed that the rate of electron-holes escaping from their recombination should be proportional to the light flux of excitation and to the probability of light absorption to produce an electron-hole couple (F). This means that the optimal dosage may be dependent on the reaction conditions. The value of F under visible light illumination is much lower than that under UV illumination in this study. The lower F value might lead to a lower Ti^{3+} content. Therefore, the optimal dosage of ceria under visible light illumination is lower than that under UV illumination at these experimental conditions.

2.2 The effect of co-doping on the photocatalytic activity

Xu *et al.* [25] have prepared Ce, C-codoped TiO_2 nanoparticles through a modified sol–gel method under mild conditions and have studied their photocatalytic activity under visible light. The UV–vis spectra of the TiO_2 samples (plotted in Fig. 5) show that Ce, C-codoped titania has a greatly improved absorption of visible light.

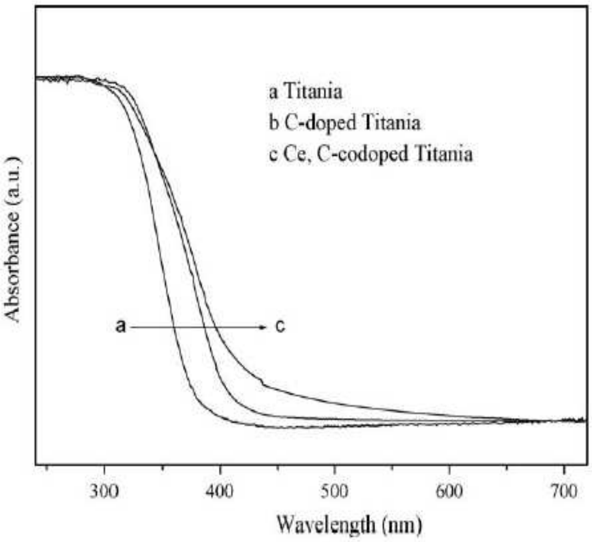

Fig. 5. UV-Vis spectra of Ce, C-codoped titania particles [25].

The authors claim that the distance of charge transfer between the ***f***-electrons of the cerium ions (or the C dopant) and the conduction or valence band of TiO_2 is narrowed, thus allowing visible light absorption. The energy level of Ce^{4+}/Ce^{3+} is 1.8 eV. The introduction of such energy level in the band-gap can give rise to the red-shift in the band-gap transition. The Ce 4***f*** level also plays an important role in the interfacial charge transfer and elimination of the electron-hole recombination.

2.3 Shift of the absorption from the UV region to the visible light region by organic dye sensitizing

Xie and Yuan [26] have demonstrated an effective photodegradation of reactive brilliant red dye (X-3B) with the reaction system dye/Ce^{4+}-TiO_2/visible-light prepared by chemical coprecipitation–peptization and hydrothermal synthesis. The optical band gap energy of TiO_2 sol is estimated to be 350 nm by measuring the UV-Vis spectra for TiO_2 and Ce^{4+}-TiO_2 sol. Both TiO_2 and Ce^{4+}-TiO_2 sols have similar UV-Vis absorption spectra except for the absorption intensity at the maximum wavelength (λ_{max} = 202 nm). There was no apparent absorption in the visible-light range ($\lambda >$ 400 nm). This means that the sol–sol system cannot be directly excited by visible light irradiation. The absorption band shows a blue shift, which is due to the quantum size effect of sol nanoparticles. The experimental results, however, show that the dye photobleaching reaction occurs on Ce^{4+}-TiO_2 (both sol and nanocrystalline system) under visible light. The photosensitized photocatalysis reaction mechanism of dye bleaching in the Ce^{4+}-TiO_2 sol system is shown in Fig. 6.

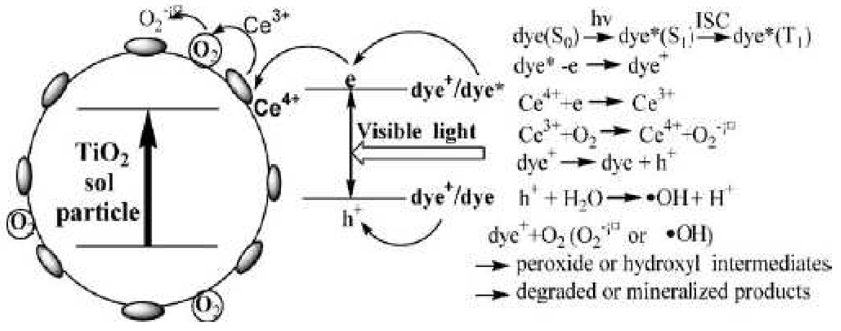

Fig. 6. Photosensitized photocatalysis mechanism of the Ce^{4+}-TiO_2 sol system [26].

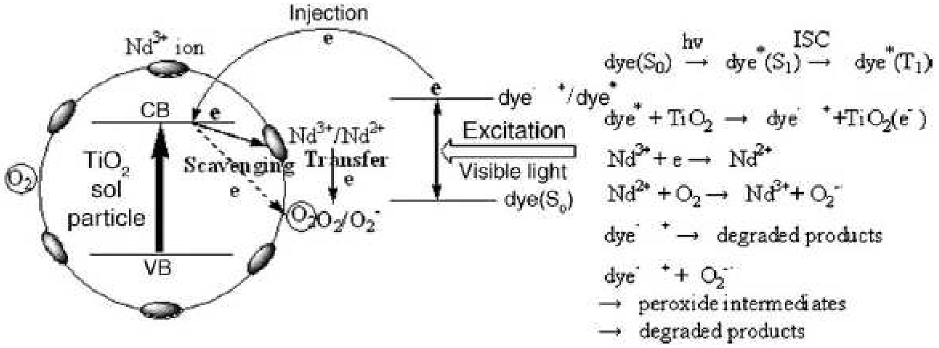

Fig. 7. Sensitized photocatalysis mechanism in the Nd^{3+}–TiO_2 sol system (S_0 = singlet ground state, S_1 = first excited singlet, T_1 = first excited triplet state, ISC = intersystem crossing) [27].

It can be seen from Fig. 6 that the Ce^{4+}-TiO_2 sol particles are physically adsorbed on the surface of sol particles and a dye molecule is excited by the absorption of a visible-light photon. The dye molecule in the excited state can then transfer electrons to the Ce^{4+} ion. Meanwhile, the positively charged vacancies (h^+) remaining on the dye molecule can extract electrons from hydroxyl species in the solution to produce hydroxyl radicals ($HO^•$). These radicals are strong electrophiles capable of oxidizing and destroying organic molecules in aqueous media. In this process, the Ce^{4+} species act as electron scavengers to trap the excitation electrons of the excited dye molecules. In this way they behave as being apparently superior to the oxygen molecule (O_2) which is also able to do that. The electrons trapped in Ce^{4+} sites are subsequently transferred to the adsorbed surrounding O_2. The presence of Ce^{4+} on the surface of sol nanoparticles may promote the following reactions: $Ce^{4+} + e^- \rightarrow Ce^{3+}$ and $Ce^{3+} + O_2 \rightarrow Ce^{4+} + O^{•-}_2$. This is then also followed by the destruction of dye molecules with the interaction of holes (h^+) and hydroxyl radicals ($HO^•$).

Xie and Yuan [27] have also studied the enhanced photocatalytic activity of active brilliant red dye X-3B in a hydrosol reaction system of Nd^{3+}–TiO_2 sol in comparison to TiO_2 sol. They have ascribed the obtained enhancement to the electron trapping effect of the modified Nd^{3+} ions on TiO_2 sol particles. The neodymium-ion modified titania sol is prepared by a chemical coprecipitation–peptization and its photoactivity is studied by investigating the photodegradation efficiency of active dye X-3B in the hydrosol reaction system. Under visible light irradiation ($\lambda > 400$ nm), Nd^{3+}–TiO_2 sol shows a higher photocatalytic activity than the TiO_2 sol, which is ascribed to the electron trapping effect of modified Nd^{3+} ions on the TiO_2 sol particles. The photosensitization-photocatalysis mechanism is also discussed; the authors have proposed that the mechanism starts with the excitation of a X-3B dye molecule with visible light, followed by electron injection or electron transfer from the excited dye molecule to the conduction band of the semiconductor TiO_2, as shown in Fig. 7.

In this sol photocatalysis system, a dye molecule physically adsorbed on the surface of a sol particle is excited by the absorption of a suitable visible light photon. The electron from the excited dye molecule can be injected into the conduction band of TiO_2. Then these electrons can be trapped by electron scavengers (usually oxygen molecules). However, the electrons are also extremely susceptible for recombination with the cation radicals if the injected electrons accumulate in the conduction band of TiO_2. Therefore, the electron trapping and electron transfer are the two key steps to inhibit electron–cation radical recombination. The cation radical ($dye^{•+}$) produced by the electron injection is less stable than the ground state of the compound (dye). As a result, the unstable cation radical of dye may either directly degrade to products or react with superoxide radical anion ($O_2^{•-}$) to produce degradation products. The photocatalysis of TiO_2 sol and P25 TiO_2 powder can be explained by the above reaction mechanism. However, in the photocatalysis with Nd^{3+}–TiO_2 sol system, the Nd^{3+} species can act as effective electron scavengers to trap the conduction band electrons of TiO_2 that have been injected from the excited dye molecules. Nd^{3+} ions, as a Lewis acid, apparently are superior to oxygen molecules (O_2) in their ability to trap electrons. The electrons trapped on Nd^{3+} sites (Nd^{2+}) are subsequently transferred to the surrounding adsorbed O_2 by an oxidation process. The presence of Nd^{3+} on the surface of TiO_2 sol nanoparticle may promote the following processes: $Nd^{3+} + e^{-} \rightarrow Nd^{2+}$ and $Nd^{2+} + O_2 \rightarrow Nd^{3+} + O_2^{\bullet -}$. More effective electron trapping and transferring will produce more cation radicals, which are more active to undergo degradation. Therefore, Nd^{3+} TiO_2 sol shows a superior photocatalytic activity in comparison with the TiO_2 sol and P25 TiO_2 powder.

Xie and Yuan [28] have also studied the activity of Nd^{3+}–TiO_2 nanocolloids for the photodegradation of phenol in water solution by visibile light, and have explained the observed enhancement with self-sensitization and sub-band gap overlapping. The AFM micrograph and XRD show that sol particles (10 nm in size) are well developed in the whole dispersion system and have a semicrystalline structure. The difference in ion radius (1.13 nm for Nd^{3+} and 0.64 nm for Ti^{4+}) means that the neodymium(III) ion is unlikely to be built effectively into the crystal lattice of bulk TiO_2 when the Nd^{3+}–TiO_2 sol crystallizes at 62°C. However, during the peptizing and digesting processes, Nd^{3+} can bond with non-bridging oxygen ions at the surface of –Ti–O–Ti–O– bulk network structure. After crystallization, the sol system forms with individual TiO_2 particles crosslinked with neodymium cations at the surface, which form NdOCl molecules. NdOCl is sensitive to visible light, but its discrete energy levels cannot be split into well divided band gaps. Due to the character of electronic arrangement of neodymium with partially filled atomic ***d*** or ***f*** shells, electrons can be excited and transferred from the Nd^{3+} $4f^3$-orbitals by absorbing visible-light photons of the right energy. The surrounding Nd^{3+} ions may react with the Nd^{4+} produced by a self-sensitization process, thus forming a positively charged neodymium cluster $(Nd_n)^{m+}$ ($m > 3n$). This neodymium cluster has empty multi energy levels below the conduction band of crystalline TiO_2. Their presence allows a new electronic transition from the TiO_2 valence band to the empty energy levels of neodymium cluster known as a sub-band gap. This transition requires less energy than the TiO_2 valence-conduction band transition (3.2 eV) and can be induced by visible light. Simultaneously, the positively charged vacancies (h^+) in the TiO_2 valence band can extract electrons from the hydroxyl species to produce hydroxyl radicals ($^{\bullet}OH$), by which organic molecules as well as other oxidizable species can be degraded. Figure 8 shows the photocatalytic reaction mechanism in the Nd^{3+}–TiO_2 sol system.

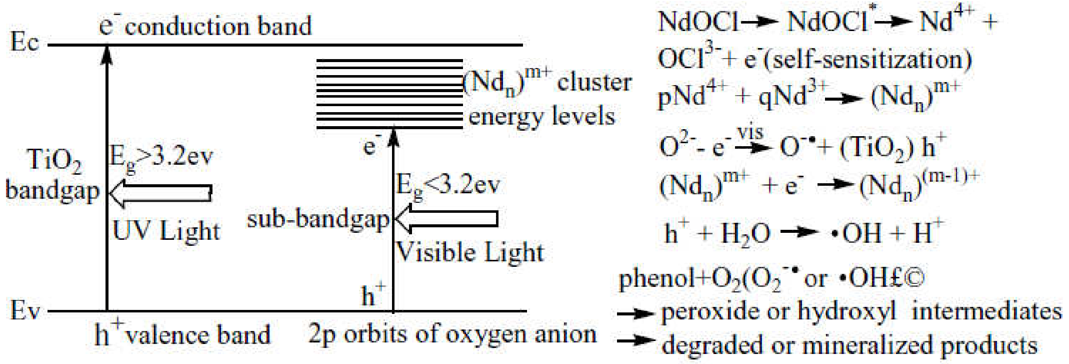

Fig. 8. Photocatalytic mechanism of Nd^{3+}–TiO_2 sol/visible light system [28].

Xie *et al.* [29] have then studied photosensitized and photocatalyzed degradation of azo dye using Ln^{n+}-TiO_2 sol in aqueous solution under visible light irradiation. They have developed a new method of chemical coprecipitation–peptization to synthesize a crystalline TiO_2 sol at a low temperature (<100°C), which is attractive to further improve the photocatalytic activity of TiO_2 catalysts. Compared to most TiO_2 powders, these TiO_2 sol catalysts have several advantages: (1) finer particle size with more uniform distribution and better dispersion in water; (2) stronger interfacial adsorption ability; and (3) easy coating on different supporting materials including substrates with a poor heat resistance such as polymers, optical fibers, plastics, wood, and paper.

It is generally believed that pure TiO_2 can not be directly excited by visible light due to its high band-gap of 3.2 eV. The system X-3B dye/Ln^{3+}-TiO_2 has an entirely different mechanism of photo-excitation under visible light illumination. The X-3B dye sensitization process involves the excitation of dye molecules by absorbing visible light photons, followed by the electron injection from excited dye molecules to the TiO_2 conduction band. Then the electrons are transferred from the conduction band to the working electrode (ITO conductive film) and finally form out-circuit. In such as system (dye/Ln^{n+}-TiO_2/vis hydrosol), the Ln^{n+}-TiO_2 particles act as a bridge band connecting the X-3B dye and the working electrode. Some key reactions are shown in Eqs. (9–14):

$$\text{Dye} + h\nu \rightarrow \text{dye}^* \quad (9)$$

$$\text{Dye}^* + TiO_2 \rightarrow TiO_2(e^-) + \text{dye}^{\bullet +} \quad (10)$$

$$TiO_2(e^-) + O_2 \rightarrow O_2^{\bullet -} + TiO_2 \quad (11)$$

$$Ln^{n+} + TiO_2(e^-) \rightarrow Ln^{(n-1)+} + TiO_2 \quad (12)$$

$$Ln^{(n-1)+} + O_2 \rightarrow O_2^{\bullet -} + Ln^{n+} \quad (13)$$

$$O_2^{\bullet -} + \text{dye}^{\bullet +} \rightarrow \text{intermediates or final products} \quad (14)$$

In the above reactions, the dye can be excited under visible light illumination (Eq. 9). The dye molecule in the excited state can then transfer electrons into the conduction band of TiO_2 (Eq. 10) that may be trapped by the electron scavengers such as oxygen molecule that usually surround the sample (Eq. 11). If the transferred electrons accumulate in the conduction band of TiO_2, recombination between cationic radicals and the electrons is extremely likely. Therefore, the electron trapping (Eq. 12) and electron transfer (Eq. 13) are two key steps to inhibit electron-cationic radical recombination. The cationic radical (dye$^{\bullet +}$) produced by electron injection is less stable than the probe molecule in the ground state. As a result, the unstable dye cationic radicals can be directly degraded into decomposition products by reacting with super-oxidizing anionic radials or other active oxygen ($HO^{\bullet}$, $HOO^{\bullet}$ and $O_2^{\bullet -}$) (Eq. 14). The lanthanide ion that TiO_2 is doped with plays an important role in promoting significantly the electron trapping and electron transfer in the dye/Ln^{3+}-TiO_2 hydrosol system. The photosensitization reaction mechanism and potential states in the dye/Ln^{n+}-TiO_2/vis system are further illustrated in Figs. 9 and 10.

Su *et al.* [30] have studied the visible light photocatalysis on praseodymium(III)-nitrate-modified nanocrystalline TiO_2 5 nm in particle diameter, that is prepared by an ultrasound method in a sol–gel process at low temperature. The UV–vis diffuse reflectance spectra of the $Pr(NO_3)_3$-TiO_2 and undoped TiO_2 samples show that both samples have a strong absorption at wavelengths below 400 nm, which is attributed to the transitions of electrons from the valence band to the conduction band of TiO_2. Visible light absorptions at 444, 469, 482 and 590 nm are observed for $Pr(NO_3)_3$-TiO_2 only, which are attributed to the 4*f*-transitions $^3H_4 \rightarrow {}^3P_2$, $^3H_4 \rightarrow {}^3P_1$, $^3H_4 \rightarrow {}^3P_0$ and $^3H_4 \rightarrow {}^1D_2$ of praseodymium(III) ions. This absorption feature suggests that the photocatalyst can be activated throughout the visible wavelengths where the light absorption occurs. The sample shows a high activity and stability in the decomposition of rhodamine-B (RhB) and 4-chlorophenol (4-CP) under visible light

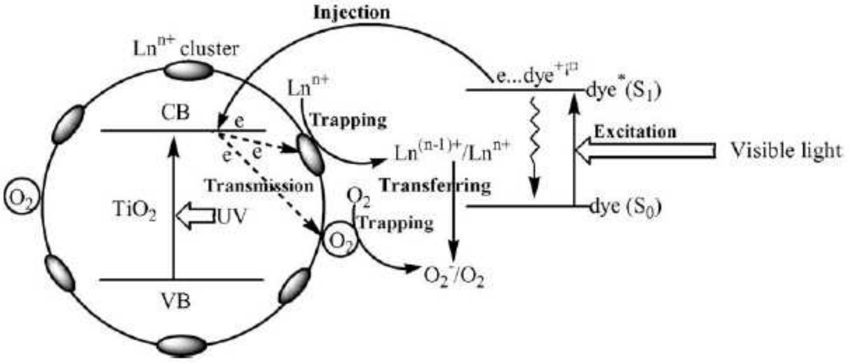

Fig. 9. Proposed mechanism of photosensitization reaction in the system dye/Ln^{n+}-TiO_2/vis [29].

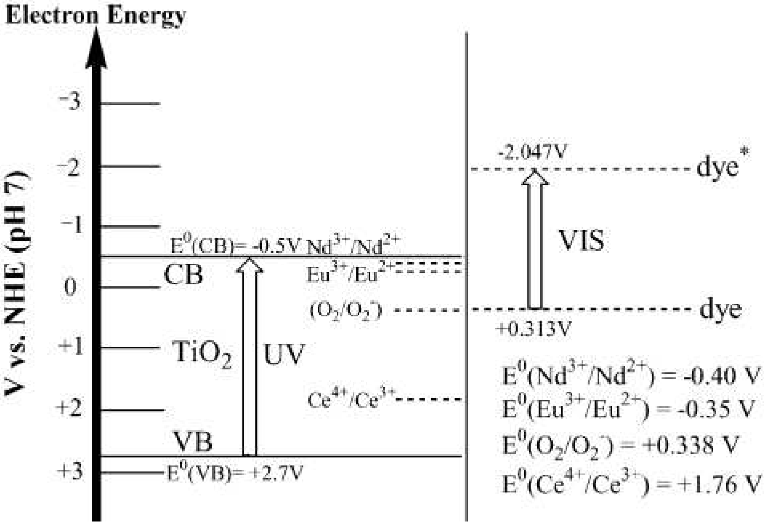

Fig. 10. Schematic illustration of the valence and conduction band potentials of TiO_2 and excitation and ground state potentials of the X-3B molecule along with the standard reduction potentials of lanthanide ion pairs [29].

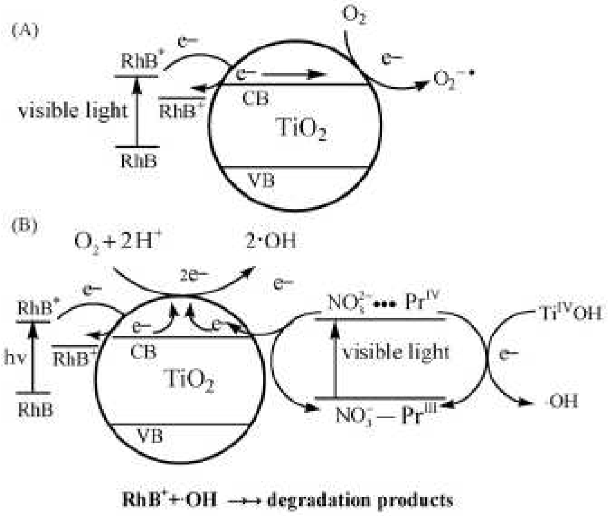

Fig. 11. Postulated mechanism for the visible light-induced oxidative degradation of RhB in aerobic aqueous media on TiO_2 (A) and $Pr(NO_3)_3$-TiO_2 (B) surfaces [30].

irradiation. From the investigation of photoinduced conversion of RhB, carried out under visible light illumination at wavelengths greater than 420 nm in aqueous $Pr(NO_3)_3$-TiO_2 dispersions, one can conclude that RhB photodegrades by a pathway that is distinct from the pathway prevailing in the pure TiO_2 dispersion. The latter pathway is related to self-photosensitization of RhB as shown in Fig. 11A.

The results presented above reveal that a completely different mechanism of charge generation must operate for the $Pr(NO_3)_3$-TiO_2 photocatalysts. The authors postulate as a working hypothesis a simple mechanism depicted in Fig. 11B. The local excitation of praseodymium(III) nitrate under visible light irradiation yields a metal-to-ligand charge-transfer transition $4f(Pr^{3+})(^3H_4 \rightarrow {}^3P_2, {}^3P_1, {}^3P_0$ and $^1D_2) \rightarrow \pi^*$ (NO_3^-), which produces Pr^{4+} and NO_3^{2-}-intermediates. The labile NO_3^{2-} anion intermediate will rapidly transfer electrons to the conduction band of TiO_2. The strong oxidizing Pr^{4+} ions (standard redox potentials of $E_0(Pr^{4+}/Pr^{3+})$ = +2.86 V, and $E_{vb}(TiO_2)$ = +2.7 V) attract electrons from either the surface OH^- groups and/or the surface H_2O molecules to produce hydroxyl radicals through the reaction depicted in Fig. 11B (evidence for this is found in the ESR spectrum). This electron transfer leads to efficient charge separation and effectively suppresses the recombination between Pr(IV) and NO_3^{2-} by the surrounding TiO_2 matrix. In the absence of $Pr(NO_3)_3$, the titania cannot be directly excited by visible light due to its 3.2 eV band-gap, but the photobleaching reaction still occurs in the TiO_2/dye/visible light system due to the dye molecule acting as a photosensitizer. Molecular O_2 adsorbed on TiO_2 acts as an electron scavenger to trap the excitation electrons of the excited dye molecules, thus producing superoxide radical $(O_2^{\bullet -})$, so that the extent of photoactivity is somewhat lessened. The difference in ESR spectra observed with respect to the kind of active oxygen species produced between the $Pr(NO_3)_3$-TiO_2 and TiO_2 dispersions is then understandable. In addition to the local excited photocatalysis, the dye assisted photosensitization also plays an important role in the photo-oxidative degradation of RhB in the dye/TiO_2 system. The produced superoxide radical is reduced by the electron from NO_3^{2-} to form $^\bullet OH$, as shown in Fig. 11B. Therefore, the photocatalysis and photosensitization simultaneously occur under visible light irradiation. It is clearly shown that the photocatalytic oxidation is superior to the photosensitized oxidation, and the photocatalytic process will surely help to improve the overall photodegradation efficiency and make the bleaching reaction more feasible.

Mele *et al.* [12] have compared the photocatalytic activity of TiO_2 samples impregnated with lanthanide diphthalocyanines with those impregnated with Cu(II)-porphyrin. The photocatalytic degradation of 4-nitrophenol (4-NP) in aqueous suspension is used as a probe reaction. Commercial anatase TiO_2 is impregnated with home-prepared double-decker phthalocyanine complexes of the lanthanide metals, such as Ce, Pr, Nd, Sm, Ho, and Gd. In particular, the impregnation with Ho, Sm, and Nd complexes, acting as sensitizers, proves beneficial for the photoactivity of studied systems. Significant improvements of the TiO_2-based catalytic system seem possible in terms of lower impregnation loading, enhanced photoreactivity under solar light irradiation, as well as chemical, thermal, and photochemical stability of the sensitizers in comparison with those using Cu(II)-porphyrin.

No appreciable shift of the band gap edge of TiO_2 can be observed for all of the samples from the diffuse reflectance spectra of bare TiO_2 and some $LnPc_2$-loaded TiO_2 photocatalysts recorded in the range of 250-800 nm. Nevertheless, all of them reflect less light than the bare support, and the absorption increases with increasing of loading. All of the spectra of the $LnPc_2$-TiO_2 samples present quite similar patterns, independent of the coordinated lanthanide metal, showing absorption maxima at nearly the same λ- value. The characteristic bands are due to the strong absorption, particularly within the Q-range (ca. 650-680 nm), by the $LnPc_2$ particles deposited on the TiO_2 grains. The bands are relatively broad compared to the respective solution spectra, and all of the studied samples show similar large absorptions that cover the visible range fairly well. Moreover, the spectra of $SmPc_2$, $GdPc_2$, and $HoPc_2$ show distinct absorption peaks at ca. 460 nm, similar to the pesaks in dichloromethane and in nujol suspension. The $LnPc_2$ sensitizers probably enhance the absorption of studied samples also within the near-UV range (ca. 300-350 nm, B band).

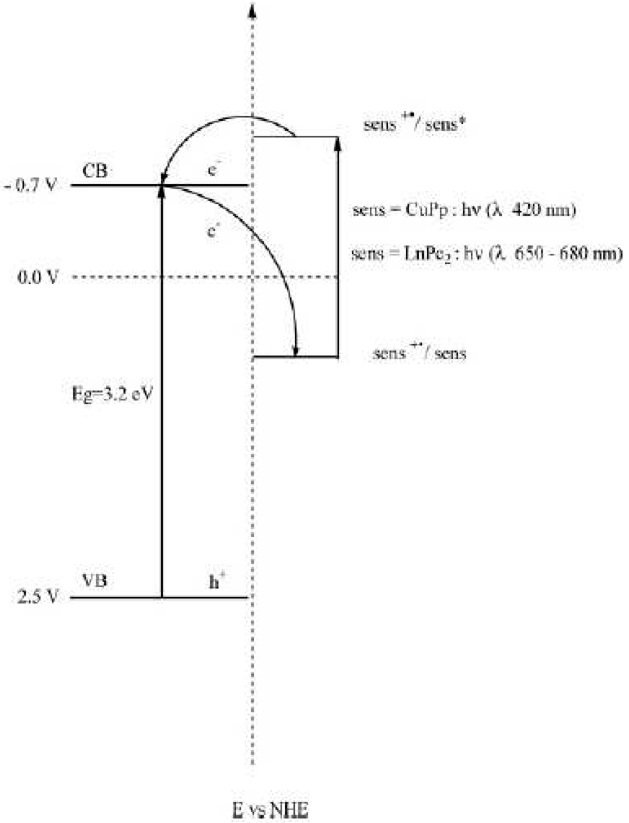

Fig. 12. Conduction Band (CB) and Valence Band (VB) energy levels of anatase TiO_2 at neutral pH and redox potentials of the various sensitizers considered in this study [12].

Figure 12 shows the conduction band and the valence band energy levels of anatase TiO_2 along with the redox potentials of some sensitizers similar to those used in this study and reported in the literature, as well as the possible charge transfer processes involving an injection of an electron from the excited sensitizers to the conduction band of TiO_2 and from the conduction band of TiO_2 to the sensitizers.

The presence of two phthalocyanine macrocycles in $LnPc_2$ favors probably a better delocalization of the positive charges during certain stages of the radical photocatalytic mechanism compared to “classic” porphyrins and phthalocyanine systems previously used as sensitizers. However, it is not easy to obtain a direct experimental evidence for this hypothesis. In addition, the formation of singlet oxygen [$^1O_2(^1\triangle)$] in higher quantities, promoted by the photoexcited $LnPc_2$ sensitizers (sens), as shown bellow by eqs 15 and 16, and suggested elsewhere, may not be excluded.

$$[\mathrm{sens}] \xrightarrow{h\nu} {}^{1}[\mathrm{sens}]^{*} \xrightarrow{\substack{\text{intersystem crossing}\\ \text{(isc)}}} {}^{3}[\mathrm{sens}]^{*} \qquad (15)$$

$${}^{3}[\mathrm{sens}]^{*} + {}^{3}\mathrm{O}_2 \rightarrow [\mathrm{sens}] + {}^{1}\mathrm{O}_2({}^{1}\Delta) \qquad (16)$$

3. CONCLUSIONS

This review presents a summary of the attempts made by different researchers in the past decades to shift the absorption of TiO_2 from UV-light to the visible light region by lanthanide doping. To understand the factors, by which TiO_2 doping by lanthanides can increase the photocatalytic activity under solar irradiation, the first chapter presents brieflly the physical mechanisms responsible for the degradation of organic pollutants by lanthanide oxide doped titania under UV-light exposure. Some typical examples are presented, where the enhancement of photocatalytic activity of TiO_2 powder is due to the suppression of electron-hole recombination with trapping of photogenerated electrons at the interface, the different effects of mesoporous wall, the co-doping and the intrinsic surface properties. Based on these findings, the second chapter presents the ways of increasing the photocatalytic activity of catalysts under visible-light exposure. The shift of photocatalytic activity of catalysts towards visible-light by bathochromic shift, co-doping and organic dye sensitizing of lanthanide oxide doped titania are presented.

Acknowledgments. *This study was performed with the financial support of the NATO "Science for Peace" Programme (Contract SfP 982835) as well of project DO02-252 of the National Science Fund of Bulgaria. The authors are thankfull to Dr. C. Dushkin (Faculty of Chemistry, University of Sofia) and Dr. R. Smits (Catalysis Services International, Sofia) for the valuable discussions.*

REFERENCES

1. A. Fujishima, K. Honda, *Nature*, **238**, 37 (1972).
2. M. R. Hoffmann, S. T. Martin, W. Choi, D. W. Bahnemannt, *Chem. Rev*., **95**, 69 (1995).
3. A. M. Volodin, *Catal. Today*, **58**, 103 (2000).
4. T. Kako, Z. Zou, M. Katagiri, J. Ye, Chem. Mater., **19**, 198 (2007).
5. C. A. Koval, J. N. Howard, *Chem. Rev.,* **92**, 411(1992).
6. Z. Zhao Q. Liu, *J. Phys. D: Appl. Phys.,* **41**, 085417 (2008).
7. J. L. Gole, J. D. Stout, C. Burda, Y. Lou, X. Chen, *J. Phys. Chem. B,* **108**, 1230 (2004).
8. Z. Li, H. Xue, X. Wang, X. Fu, *J. Molec. Catal. A: Chem.*, **260**, 56 (2006).
9. S. Rengaraj, S. Venkataraj, Jei-Won Yeon, Y. Kim, X.Z. Li, G.K.H. Pang, *Appl. Catal. B: Env.,* **77**, 157 (2007).
10. A. Scalfani, J.M. Hermann, *J. Photochem. Photobiol. A*, **113**, 181(1998).
11. H. Yang, K. Zhang, R. Shi, A. Tang, *J. Am. Ceram. Soc*., **90**, 1370 (2007).
12. G. Mele, E. García-López, L. Palmisano, G. Dyrda, R. Słota, *J. Phys. Chem. C*, **111**, 6581 (2007).
13. H. Q. Jiang, P. Wang, X. L. Guo, and H. Z. Xian, *Rus. Chem. Bull.*, **55**, 1743 (2006).
14. A. N. Ökte, Ö. Yılmaz, *Appl. Catal. A: Gener.* **354** 132 (2009).
15. T. Peng, De Zhao, H. Song, C. Yan, *J. Molec. Catal. A: Chem.,* **238,** 119 (2005).
16. De Zhao, T. Peng, J. Xiao, C. Yan, X. Ke, *Mater. Lett.,* **61,** 105 (2007).
17. J.-W. Shi, J.-T. Zheng, Y. Hu, Y.-C. Zhao, *Mater. Chem. Phys.,* **106,** 247 (2007).
18. L. Zhang, H. Zhong, W. Zhang , L. Lu, X. Yang, X. Wang, *J. Alloy. Comp.*, **463,** 466 (2008).
19. K. M. Parida, N. Sahu, *J. Molec. Catal. A: Chem.,* **287**, 151 (2008).
20. Q. Xiao, Z. Si, Z. Yu, G. Qiu, *Mater. Sci. Eng.* B, **137**, 189 (2007).
21. F. B. Li, X. Z. Li, M. F. Hou, K.W. Cheah, W. C .H. Choy, *Appl. Catal. A: Gen.*, **285**, 181 (2005).
22. B. Elidrissi, M. Addou, M. Regragui, C. Monty, A. Bougrine, A. Kachouane, *Thin Solid Films,* **379,** 23 (2000).
23. S.Y. Zheng, A. M. Andersson-Faldt, C. G. Granqvist, *Appl. Opt.*, **32**, 6303 (1993).
24. S. Ikeda, N. Sugiyama, B. Pal, G. Marci, L. Palmisano, H. Noguchi, K. Uosaki, B. Ohtani, *Phys. Chem. Chem. Phys.*, **3**, 267 (2001).
25. J. Xu, Y. Ao, D. Fu, *Appl. Surf. Sci.*, **256,** 884 (2009).
26. Y. Xie, C. Yuan, App. Catal. B: Envir., **46**, 251 (2003).
27. Y. Xie, C. Yuan, X. Li, *Coll. Surf. A: Physicochem. Eng. Aspects*, **252**, 87 (2005).
28. Y. Xie, C. Yuan, *Appl. Surf. Sci.*, **221**, 17 (2004).
29. Y. Xie, C. Yuan, X. Li, *Mater. Sci. Engin. B*, **117**, 325 (2005).
30. W. Su, J. Chen, L. Wu, X. Wang, X. Wang, X. Fu, Appl. *Catal. B: Envir.*, **77**, 264 (2008).

ТИТАНОВ ДИОКСИД С ДОБАВКИ ОТ ЛАНТАНОИДИ КАТО ФОТОКАТАЛИЗАТОР ЗА РАЗГРАЖДАНЕ НА ОРГАНИЧНИ ЗАМЪРСИТЕЛИ ПРИ ОБЛЪЧВАНЕ С УЛТРАВИОЛЕТОВА И ВИДИМА СВЕЛИНА

Д. Ц. Димитров*, М. М. Миланова, Р. П. Кралчевска

Катедра Обща и неорганична химия, Химически факултет,Софийски университет, бул. Джеймс Баучър 1, София 1164, България

Постъпила на 2 Ноември 2010 г.; Преработена на 5 януари 2011 г.

(Резюме)

Основната цел поставена при написването на този кратък обзор е да представи най-значимите изследвания, които бяха проведени през последните десетилетия, свързани с изместването на поглъщането на TiO_2 от ултравиолетовата във видимата област чрез добавки от лантаноиди. С цел да се внесе ясност в другите фактори, чрез които внасянето на лантаноиди в TiO_2 увеличава неговата фотокаталитична активност при облъчването му с видима светлина, първата част на обзора е посветена на физическите механизми, причиняващи разграждането на органични замърсители от модифициран с лантаноиди TiO_2 при облъчването му с ултравиолетова светлина. Тази тема е изследвана много по-отдавна и по-добре изучена. Втората част на представения обзор представя отново тези механизми, но при облъчване на катализатора с видима светлина. Там подробно са разгледани най-типичните изследвания свързани с намаляването на ширината на забранената зона на TiO_2, ефекта на съвместното модифициране едновременно с две добавки и ефекта на сенситизирането с помощта на органични оцветители при модифицираният с лантаноиди титанов диоксид.